Nuclear excitation by electron transition rate confidence interval in a ^{201}Hg local thermodynamic equilibrium plasma

M. Comet,* G. Gosselin, V. Méot, P. Morel, and J.-C. Pain
CEA, DAM, DIF F-91297 Arpajon, France

D. Denis-Petit, F. Gobet, F. Hannachi, M. Tarisien, and M. Versteegen
Université de Bordeaux, CNRS-IN2P3, CENBG, F-33175 Gradignan, France

(Received 22 July 2015; published 11 November 2015)

Nuclear excitation by electron transition (NEET) is predicted to be the dominant excitation process of the first ^{201}Hg isomeric state in a laser heated plasma. This process may occur when the energy difference between a nuclear transition and an atomic transition is close to zero, provided the quantum selection rules are fulfilled. At local thermodynamic equilibrium, an average atom model may be used, in a first approach, to evaluate the NEET rate in plasma. The statistical nature of the electronic transition spectrum is then described by the means of a Gaussian distribution around the average atom configuration. However, using a continuous function to describe the electronic spectrum is questionable in the framework of a resonant process, such as NEET. In order to get an idea of when it can be relied upon to predict a NEET rate in plasma, we present in this paper a NEET rate calculation using a model derived from detailed configuration accounting. This calculation allows us to define a confidence interval of the NEET rate around its average atom mean value, which is the first step to design a future experiment.

DOI: 10.1103/PhysRevC.92.054609 PACS number(s): 33.25.+k, 25.30.−c, 23.20.−g

I. INTRODUCTION

The understanding of the mechanisms to populate and depopulate nuclear excited states in plasma is of paramount interest to fundamental and applied aspects of nuclear science. From diagnostics of hot dense plasmas to production of an inverse population of nuclear levels, excitation of nuclei in plasma has raised renewed interest in the scientific community with the advent of intense lasers. Nuclear excitation in plasma processes has been predicted a long time ago [1,2] and still has not been observed in an experiment. Several attempts have been made [3–7], but so far none have been successful. Several excitation processes may contribute. Some involve particles from the plasma, such as photons with photoexcitation or free electrons with inelastic electron scattering [8] and nuclear excitation by electron capture [9].

One of the most promising processes is nuclear excitation by electron transition (NEET) [10]. NEET has already been observed in an accelerator-based experiment on nonplasma targets of ^{193}Ir [11], ^{189}Os [12], and ^{197}Au [13]. In none of these experiments were the atomic configurations close to those encountered in a plasma environment. Because the NEET rate depends on the electronic configuration, the NEET probability can be enhanced by modifying the atomic environment of the nucleus. In hot dense plasmas, the thermodynamic conditions strongly affect the electronic environment of the ions. Thus, plasmas are ideal laboratories to observe these modifications of nuclear rates. The NEET resonant feature lets us expect higher transition rates [14] provided that a suitable candidate nucleus can be found. ^{201}Hg is one of those few candidates as it has a low $M1/E2$ low-lying isomer at 1.565 keV with a relatively long half-life of 81 ns [15] (see Fig. 1) compared to the few nanosecond duration of a plasma heated by a laser. Sakabe *et al.* [16] predicted the $4s_{1/2}$-$3d_{3/2}$ atomic transition is resonant with the nuclear transition of a singly ionized atom. For higher charge states, transitions between $n = 6$ and $n = 4$ atomic shells conveniently lie very close to a 1.565-keV transition energy [15]. Due to the extremely low width of the nuclear transition, resonant transition rates are significantly harder to predict as a precise knowledge of atomic transition energies is required. This kind of precision is currently out of reach of all atomic physics models, and thus approximations are required.

However, for heavy nuclei, this situation can be less dramatic. Indeed, the large number of atomic configurations is the origin of a huge number of electronic transition lines which can be statistically regrouped under a small number of broadened transitions. This is the basis of the ISOMEX model [8,10,14], which relies on the relativistic average atom model (RAAM) as will be detailed in Sec. II. Its main feature is that populations of atomic shells are nonintegers, which might result in an average atom quite far from the true atom. The RAAM has the considerable advantage of its simplicity allowing for making calculations in any plasma condition. The statistical nature of the electronic spectrum can be taken into account by using a Gaussian distribution of transitions around the transition given by the RAAM. However, the use of a continuous function to describe the electronic spectrum is questionable in the framework of a resonant process, such as NEET. In order to get an idea of when it can be relied upon to predict a NEET rate in plasma, a more sophisticated approach can be used, such as detailed configuration accounting (DCA). This method will allow estimating a confidence interval of the NEET rate around its mean value. However, a proper DCA calculation requires diagonalizing the Hamiltonian operator in each configuration subspace, which is a very time-consuming

*Corresponding author: maxime.comet@cea.fr

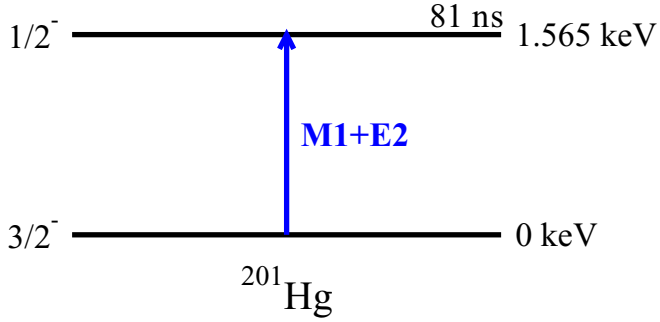

FIG. 1. (Color online) Partial level scheme of ^{201}Hg.

process. In Sec. III of this paper we propose evaluating the energy of each configuration using quantities obtained in the framework of the RAAM but with true integer populations. This will considerably lower computing times, making it a viable alternative for allowing the study of NEET rates as a function of thermodynamic conditions. Comparison of NEET rates calculated with the DCA and RAAM model will help to determine regions in the density-temperature plane where predictions performed by the RAAM are relevant. Finally, we will show that the uncertainties in the calculation of atomic transition energies are likely to enhance the difficulty to make an accurate prediction of the NEET rate and that only a confidence interval of the NEET rate around its mean value can be given.

In the long haul, these calculations will be used to design a laser experiment. In laser-created plasmas, propagation of the laser beam in the plasma is possible only below a limiting density, the so-called critical density which, for a wavelength of 1.06 μm, is around 10^{-2} g cm^{-3}. The laser deposits most of its energy at this density; therefore, most of the results presented in this paper have been performed around this density. Moreover, in the present case, the plasma is assumed to be in local thermodynamic equilibrium (LTE): The density is high enough to thermalize the plasma by electron-ion collisions whereas the photons may still escape from it. It is possible to locally define a temperature and a density, and the probabilities of the atomic level occupations and configuration probabilities can be calculated using a Fermi-Dirac distribution and Boltzmann's law.

II. THE AVERAGE ATOM MODEL

The average atom model we use is similar to the one proposed by Rozsnyai [17]. In this model, the average atom is a fictitious atom whose properties are the average atomic properties of all atoms in plasma. This model solves the Dirac equation for bound electrons with boundary conditions on the wave functions dictated by plasma density. Fractional populations of electronic shells are determined by a Fermi-Dirac statistics under the thermodynamic equilibrium hypothesis. For given plasma temperature and density, this model delivers several quantities, such as the average wave functions, populations or charge state, the latter being plotted as a function of temperature in Fig. 2 for densities of 10^{-3} and 10^{-2} g cm^{-3}.

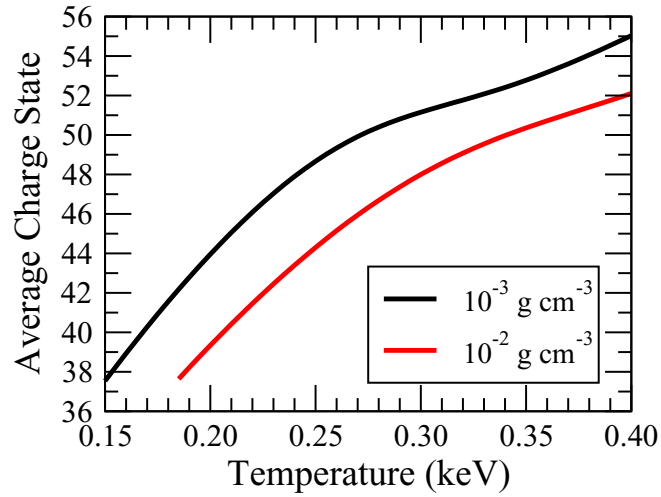

FIG. 2. (Color online) The RAAM average charge state of ^{201}Hg at 10^{-3} and 10^{-2} g cm^{-3} as a function of plasma temperature.

In the present paper, we neglect dynamical screening and many particle effects. The first one is known to have an impact on the radiative spectra [18], through channel mixing and configuration interaction. A proper description of dynamic screening would require a full quantum-mechanical description of both bound and free electronic states [19] and the use of Green's function approaches or related techniques. Such formalisms are not included in our model. Nevertheless, their impact on the NEET rate is expected to be much smaller than other approximations of the statistical methods used here. In addition, investigating multicenter effects would imply a breakdown of the average-atom picture in the central field model. However, such effects should not play a significant role in the plasmas we consider since they are mostly important for dense strongly coupled plasmas.

A. Average transition energy

To evaluate a NEET rate under plasma conditions with the RAAM, the key parameter is the average atomic transition energy, which should be as close as possible to the nuclear one. Its expression has been slightly improved from the expression previously used in Ref. [10].

In the RAAM, it is not straightforward to define the average transition energy between two configurations because the atom is described by a single average configuration. For our purpose we calculate the average transition energy by considering real electronic configurations. During a NEET transition, an electron is transferred from orbital α to orbital β between initial and final configurations C_i and C_f,

$$\begin{aligned} C_i &= (n_1\ell_1 j_1)^{N_1}(n_2\ell_2 j_2)^{N_2}\cdots(n_\beta\ell_\beta j_\beta)^{N_\beta}\cdots(n_\alpha\ell_\alpha j_\alpha)^{N_\alpha}, \\ C_f &= (n_1\ell_1 j_1)^{N_1}(n_2\ell_2 j_2)^{N_2}\cdots(n_\beta\ell_\beta j_\beta)^{N_\beta+1}\cdots \\ &\quad (n_\alpha\ell_\alpha j_\alpha)^{N_\alpha-1}, \end{aligned} \tag{1}$$

where n_k and ℓ_k, respectively, are the principal quantum number and the orbital momentum of orbital $k, j_k = \ell_k \pm 1/2$, and N_k is its integer population. The energy of any

configuration C can be calculated by [20]

$$E(C) = \sum_k N_k U_k + \frac{1}{2}\sum_k \sum_{k'} N_k(N_{k'} - \delta_{kk'})V_{kk'} + \sum_k N_k V_{k\ell}, \quad (2)$$

where U_k contains the kinetic energy and the electron-nucleus interaction of the electron in the k orbital, $V_{kk'}$ is the bound-bound electron interaction energy, and $V_{k\ell}$ is the free-bound interaction under the Thomas-Fermi approximation [21,22]. Free-free interactions have been neglected as they do not play a significant part when dealing with NEET transitions which involve bound-bound atomic transitions. In the RAAM, these energies are replaced by their average values, and the transition energy can be easily deduced

$$h\nu_{\alpha\to\beta} = (\bar{U}_\alpha - \bar{U}_\beta) - (\bar{V}_{\alpha\alpha} - \bar{V}_{\beta\alpha}) + \sum_k N_k(\bar{V}_{\alpha k} - \bar{V}_{\beta k}) + (\bar{V}_{\alpha\ell} - \bar{V}_{\beta\ell}). \quad (3)$$

Relation (3) can be reexpressed as

$$h\nu_{\alpha\to\beta} = \overline{h\nu}_{\alpha\to\beta} + \sum_k (\bar{V}_{\alpha k} - \bar{V}_{\beta k})(N_k - \bar{N}_k), \quad (4)$$

where $\overline{N}_k$ is the average noninteger population and $\overline{h\nu}_{\alpha\to\beta}$ is the average atomic transition energy,

$$\overline{h\nu}_{\alpha\to\beta} = (\bar{U}_\alpha - \bar{U}_\beta) - (\bar{V}_{\alpha\alpha} - \bar{V}_{\beta\alpha}) + \sum_k (\bar{V}_{\alpha k} - \bar{V}_{\beta k})\bar{N}_k + (\bar{V}_{\alpha\ell} - \bar{V}_{\beta\ell}). \quad (5)$$

The main difference with the expression published in Ref. [10] lies in the averaging process and the inclusion of the free-bound interaction. Here averaging is restricted to configurations with at least an electron in orbital α and a hole in orbital β. This expression provides a better result for radiative spectrum calculation. The transition energy difference between expression (5) and its old counterpart [10] is around 10 eV in the ^{201}Hg transitions of interest and could be up to 100 eV if inner shells were involved.

B. NEET rate within the average atom model

The influence of the huge number of electronic configurations on the average transition energy is taken into account by a Gaussian-shaped broadening around the average transition energy [22]. Coupled with the RAAM, this NEET rate evaluation model will be labeled as average atom Gaussian (AAG) in this paper. This gives a NEET rate from initial orbital α to final orbital β [10],

$$\bar{\lambda}^{\mathrm{NEET}}_{\alpha\to\beta}(\rho,T) = \frac{2\pi}{\hbar}\bar{N}_\alpha(1-\bar{p}_\beta)|\bar{W}_{\alpha\beta}|^2 \frac{1}{\sqrt{2\pi}\sigma_{\alpha\beta}} \exp\left(-\frac{\bar{\delta}^2_{\alpha\beta}}{2\sigma^2_{\alpha\beta}}\right), \quad (6)$$

where ρ and T, respectively, are the density and the temperature of the plasma, $\bar{p}_\beta = \bar{N}_\beta/g_\beta$ is the average probability of occupation in the final orbital β defined as the ratio between the average population $\bar{N}_\beta$ and the degeneracy g_β, and $\bar{\delta}_{\alpha\beta}$ is the average mismatch defined as the energy difference between the average atomic and nuclear (ΔE_{nuc}) transition energies,

$$\bar{\delta}_{\alpha\beta} = \overline{h\nu}_{\alpha\to\beta} - \Delta E_{\mathrm{nuc}}. \quad (7)$$

$|\bar{W}_{\alpha\beta}|^2$ is the squared nucleus-atom matrix coupling element [10] whose expression is given, for a πL electromagnetic transition by

$$|\bar{W}_{\alpha\beta}|^2 = 4\pi e^2 k_N^{2L+2}\left\langle j_\alpha L\frac{1}{2}0\middle| j_\beta\frac{1}{2}\right\rangle^2 \frac{1}{[L(2L+1)!!]^2} \times |\bar{R}_{\alpha\beta}(\pi L)|^2 B_{g\to e}(\pi L), \quad (8)$$

where e is the electron charge, k_N is the wave number associated with the nuclear transition, $B_{g\to e}(\pi L)$ is its reduced transition probability from the ground (g) to the excited (e) state, and $\bar{R}_{\alpha\beta}(\pi L)$ is the radial integral.

For an electric transition, the radial integral is as follows:

$$\bar{R}_{\alpha\beta}(EL) = \int_0^\infty \{L(\bar{P}_\alpha\bar{P}_\beta + \bar{Q}_\alpha\bar{Q}_\beta)h_L(k_N r) + [(\kappa_\alpha - \kappa_\beta - L)\bar{P}_\alpha\bar{Q}_\beta + (\kappa_\alpha - \kappa_\beta + L)\bar{Q}_\alpha\bar{P}_\beta] \times h_{L-1}(k_N r)\}dr, \quad (9)$$

and for a magnetic transition,

$$\bar{R}_{\alpha\beta}(ML) = (\kappa_\alpha + \kappa_\beta)\int_0^\infty [\bar{P}_\alpha\bar{Q}_\beta + \bar{Q}_\alpha\bar{P}_\beta]h_L(k_N r)dr. \quad (10)$$

κ_α and κ_β are the relativistic quantum numbers of orbitals α and β whose wave-function large and small components are denoted by $\bar{P}$ and $\bar{Q}$, and h_L is Hankel's function of the first kind and of the order L [23].

$\sigma_{\alpha\beta}$ is the Gaussian standard deviation [21],

$$\sigma_{\alpha\beta} = \sum_k \sum_{k'} (\bar{V}_{\alpha k} - \bar{V}_{\beta k})(w^{-1})_{kk'}(\bar{V}_{\alpha k'} - \bar{V}_{\beta k'}), \quad (11)$$

where the w matrix is defined by [21]

$$w_{kk'} = \frac{\bar{V}_{kk'}}{k_B T} + \frac{\delta_{kk'}}{\bar{N}_k(1-\bar{p}_k)}. \quad (12)$$

Equation (12) behavior can be easily apprehended in two extreme cases. At very low temperature ($T \to 0$), the electronic configuration gets closer to the fundamental one, so the standard deviation on the electronic occupation is minimal. For the highest temperatures ($T \to \infty$), the electrostatic interaction between electrons is minimal: The standard deviation becomes larger because electrons can occupy all available states.

Figure 3 shows the NEET rate as a function of either temperature (a) or average charge state (b) at 10^{-2} g cm^{-3} for the four main contributing atomic transitions. The total NEET rate includes these four transitions and all other transitions otherwise not represented.

Two regions exhibit a higher NEET rate between 10^3 and 10^4 s^{-1}: around 230–240-eV plasma temperature ($\bar{Q} \approx 42^+$) at about $7 \cdot 10^3$ s^{-1} and around 340 eV ($\bar{Q} \approx 50^+$) with a slightly higher NEET rate at $9 \cdot 10^3$ s^{-1}. Four resonant

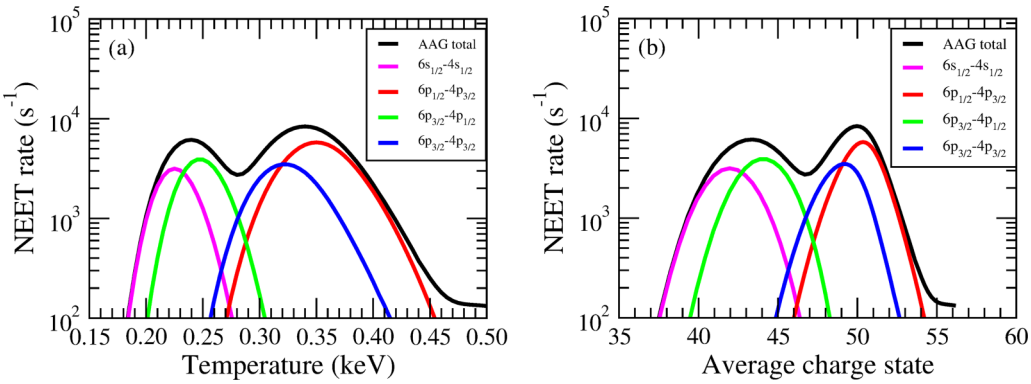

FIG. 3. (Color online) NEET rate as a function of (a) the temperature and (b) the average charge state calculated with the AAG model at 10^{-2} g cm^{-3}.

transitions contribute most of the NEET rate: $6s_{1/2}$-$4s_{1/2}$ and $6p_{3/2}$-$4p_{1/2}$ for charge states between 42^+ and 44^+ and $6p_{3/2}$-$4p_{3/2}$ and $6p_{1/2}$-$4p_{3/2}$ for 49^+ and 50^+. Modifications of the transition energy in expression (5) do not change substantially the results obtained with the model described in Ref. [10] and used in Refs. [14,15].

This calculation can be expanded to encompass the whole density-charge state plane as shown in Fig. 4.

White sectors above or below the map either have not been calculated or lie outside the temperature range of interest. The NEET rate exhibits a general increase as a function of density. For higher densities, a higher temperature is required to get the same charge state, which gives a higher number of electrons in the NEET initial atomic subshell. On top of this global increase in the NEET rate as a function of density, both sets of resonant transitions can be clearly seen. The average charge state of their maximum slowly decreases as a function of density. This behavior is consistent with thermodynamic variations of the resonance conditions as was shown in Ref. [10]. Anyway resonant average charge states do not vary much for densities around 10^{-2} g cm^{-3}, which is the critical density reached in a laser experiment. Such a map will be a useful tool if coupled to a hydrodynamic code to predict a number of nuclei excited by NEET in a laser shot with an appropriate correction [24] in order to include deviations from the LTE.

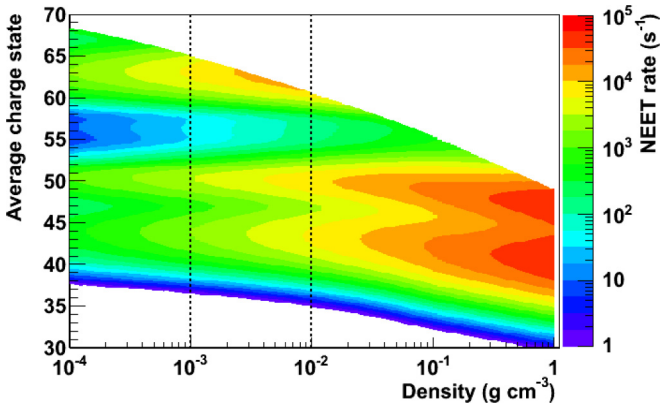

FIG. 4. (Color online) NEET rate map with the AAG model in an LTE plasma. Dotted lines are the two thermodynamical regions that will be detailed in the following to check the validity of the AAG model for NEET rate calculations.

This map has been built under the AAG model hypothesis. In next part, we will detail where on this density-temperature plane the AAG model can be trusted and where its validity can be questioned based on two calculations performed at densities of 10^{-3} and 10^{-2} g cm^{-3} (dotted lines in Fig. 4).

III. NEET RATE BEYOND THE AVERAGE ATOM MODEL

A. Model description

The AAG model assumes that the electronic spectrum is described by a continuous function, in other words that the average separation in energy between the most intense transitions is much smaller than their width. If this assumption is probably more valid for high-density plasmas and low charge states, for expanded plasma it is generally not fulfilled even at critical density. So an estimation of the uncertainty due to this hypothesis is required. This obvious limitation of the AAG model is its continuous approach to describe a resonant process. In this context, a DCA method can allow estimating the variation of the NEET rate due to uncertainties on both the nuclear and the atomic transition energies. The aim of this paper is not to develop a more efficient model but to evaluate something akin to an error bar around the average atom NEET rate and thus to obtain a confidence interval around the average atom prediction.

DCA computing times can quickly become unmanageable when dealing with charge states as low as 40^+ in mercury. Therefore, the energy of an electronic configuration is evaluated as in Eq. (2) with average values of U_k, $V_{kk'}$, and $V_{k\ell}$,

$$E(C) = \sum_k N_k \overline{U}_k + \frac{1}{2}\sum_k \sum_{k'} N_k (N_{k'} - \delta_{kk'}) \overline{V}_{kk'} + \sum_k N_k \overline{V}_{k\ell}, \quad (13)$$

where now N_k is the integer population in the k orbital. This is equivalent to approximating that all atomic configurations are calculated within the same average electronic potential which is also used to derive the average wave functions required to calculate the atom nucleus matrix coupling element. Thus all

configuration energies are calculated using the Hamiltonian operator of the average atom and not of the real configuration. Transition energy from initial orbital α to final orbital β is still calculated by the energy difference between the initial and the final configurations,

$$h\nu^{i}_{\alpha\to\beta} = E\left(C_i^{\alpha\beta}\right) - E\left(C_f^{\alpha\beta}\right). \tag{14}$$

There is now one different transition energy for each available initial configuration C_i, hence the notations $h\nu^{i}_{\alpha\to\beta}$ and $C_i^{\alpha\beta}$. The final configuration $C_f^{\alpha\beta}$ is unequivocally defined by initial configuration $C_i^{\alpha\beta}$ and α to β transition.

Individual configuration probabilities are calculated with the grand canonical partition function as the number of bound electrons changes with each configuration,

$$P(C) = \frac{g_C \exp\left[-\frac{E(C)-\mu\sum_k N_k}{k_B T}\right]}{\sum_j g_{C_j} \exp\left[-\frac{E(C_j)-\mu\sum_k N_{k,j}}{k_B T}\right]}. \tag{15}$$

g_C is the statistical weight of configuration C, μ is the chemical potential that outcomes from the RAAM calculation of electroneutrality, and E is the configuration energy. The introduction of the bound-free electron interaction in Sec. II A has a more significant effect on these probabilities as on the atomic transition energy.

The method exposed in this paper has been named ADAM (French acronym for *au-delà de l'atome moyen*, which can be translated into beyond average atom). It combines a DCA calculation with quick computing times as the electronic potential, and the atomic wave functions are only calculated once for each density and temperature couple instead of once per configuration.

B. Configuration selection

Even with reduced computing times, high-Z ions with large numbers of bound electrons still represent a challenge. A configuration selection is therefore mandatory in order to restrict calculations to a smaller number of configurations that really matter. The RAAM provides tools for this.

The first restriction consists in allowing electrons populating only a limited number of atomic orbitals. In this paper, the NEET transitions involve electrons transiting from the $n = 6$ to the $n = 4$ shells. Therefore electrons are allowed to populate all orbitals up to and including the $n = 6$ shell.

Configurations are first selected according to their charge states by restricting the charge state to be not too far away from the average,

$$\bar{Q} - \delta Q \leqslant Q \leqslant \bar{Q} + \delta Q. \tag{16}$$

In most cases adopting $\delta Q = 3$ encompasses around 99% of the total charge state distribution.

We further restrict population on each subshell by allowing only a small variation of the subshell population around the average value from the RAAM,

$$\bar{N}_k - \eta\sigma_k \leqslant N_k \leqslant \bar{N}_k + \eta\sigma_k, \tag{17}$$

where σ_k is the standard variation of the population of orbital k. An upper value for this parameter can be derived under the hypothesis of independent particles by a binomial variance,

$$\sigma_k^2 = g_k \bar{p}_k (1 - \bar{p}_k), \tag{18}$$

where g_k is orbital k degeneracy and $\bar{p}_k$ is its average probability. The parameter η has been chosen at a value of 3. Larger values have been considered in this paper [24], but they do not significantly alter the results presented hereafter.

In most cases, the configuration number is still too large, and further restrictions must be enforced. Each configuration probability is given by the above Eq. (15), but it cannot be evaluated for a given configuration without the knowledge of all other configuration energies. However an estimation of this probability can be derived from the RAAM with a binomial distribution,

$$P_B(C) = A_{\text{norm}} \prod_{k=1}^{N_{\text{orb}}} \binom{g_k}{N_k} \bar{p}_k^{N_k} (1 - \bar{p}_k)^{g_k - N_k}, \tag{19}$$

where N_{orb} is the total number of orbitals and A_{norm} is a normalization constant. This estimate can be used to select only the most probable configurations. For this purpose all configurations are sorted out by decreasing probabilities. For an atomic transition from orbital α to β, we define index i_{last} as the higher index, such as

$$\sum_{i=1}^{i_{\text{last}}} P_B\left(C_i^{\alpha\beta}\right) \leqslant (1 - \varepsilon) \sum_{i=1}^{N_{\alpha\beta}} P_B\left(C_i^{\alpha\beta}\right), \tag{20}$$

where $N_{\alpha\beta}$ is the total number of configurations allowing an α to β transition which means at least one electron in the subshell α and one hole in the subshell β. The ε coefficient has been taken at 1% in this paper in a similar way as in Ref. [25]. This selection is performed individually for each atomic transition. However one must keep in mind that the configuration probability will ultimately be calculated with the partition function through expression (15) and not by using binomial probabilities from (19). The denominator from (15) is calculated by truncating the summation with a similar criterion as (20).

C. Validation with an atomic spectrum calculation

The main advantage of the calculation method of ADAM is to avoid the resolution of the Dirac equation for each configuration. In this case, the calculation time is much shorter. To estimate the error introduced by this approach, we compare the $E2$ radiative spectrum of the $6p_{1/2}$-$4p_{3/2}$ transition calculated by ADAM to the same spectrum where the Hamiltonian of each configuration has been calculated. The total average energy of the configuration is determined by a multiconfiguration Dirac-Fock (MCDF) code [26] which implements the energy average level calculation as defined by Grant [27,29] and Bruneau [28] (this method is called here CNFM). The plasma temperature and density are chosen at 316 eV and 10^{-2} g cm^{-3}, respectively, giving a plasma average charge state of 48.88^{+}. This radiative spectrum is calculated by the relation below,

$$S^{\text{Rad}}_{\alpha\to\beta} = \sum_{C_i^{\alpha\beta}} P\left(C_i^{\alpha\beta}\right) A_{\alpha\to\beta} N_\alpha \left(1 - \frac{N_\beta}{g_\beta}\right) \Psi_{\alpha\to\beta}(h\nu), \tag{21}$$

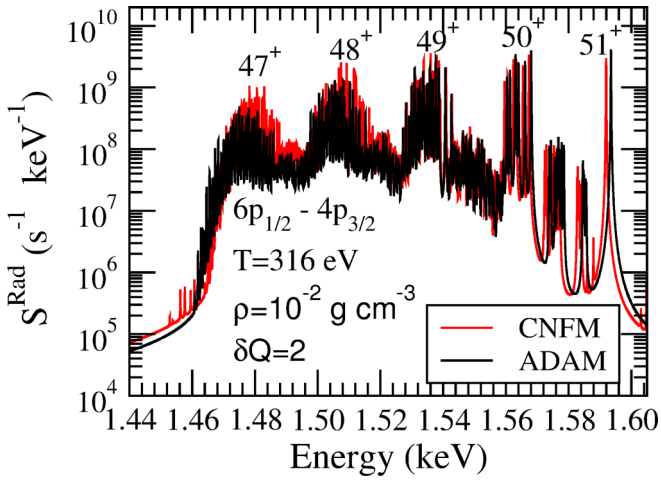

FIG. 5. (Color online) $E2$ radiative spectrum of the $6p_{1/2}$-$4p_{3/2}$ transition calculated with ADAM (black line) and in CNFM (red line) at a plasma temperature and density of 316 eV and $10^{-2}\,\mathrm{g\,cm^{-3}}$, respectively, with $\delta Q = 2$.

where N_α and N_β are the populations of orbitals α and β in configuration $C_i^{\alpha\beta}$, g_β is the β orbital degeneracy, $A_{\alpha\to\beta}$ represents the one-particle transition rate [30], and $\Psi_{\alpha\to\beta}(h\nu)$ is the transition profile. For each transition a Lorentz profile of 100-meV half-width at half maximum has been arbitrarily chosen. Figure 5 presents the $E2$ radiative spectrum of the $6p_{1/2} - 4p_{3/2}$ transition calculated by the two approaches in which the K, L, and M shells are closed.

Both spectra are very close to each other with an energy shift of a little less than 2 eV for charge states between 47^+ and 51^+ for one of the main resonant transitions: $6p_{1/2}$-$4p_{3/2}$. This can be extrapolated to lower charge states and/or to other atomic transitions at the price of longer computing times as the number of configurations rises significantly. This comparison was only performed for $\delta Q = 2$ for the sake of shortening computing times. So this pretty good agreement means using average wave functions to calculate matrix elements will not modify strongly their values.

D. NEET rate calculations

The DCA NEET rate for an atomic transition from orbital α to β is [10] as follows:

$$\lambda_{\alpha\to\beta}^{\mathrm{NEET}} = \sum_{C_i^{\alpha\beta}} P\left(C_i^{\alpha\beta}\right)\frac{\Gamma_\alpha}{\hbar}N_\alpha\left(1-\frac{N_\beta}{g_\beta}\right) \times\left(1+\frac{\Gamma_\beta}{\Gamma_\alpha}\right)\frac{|W_{\alpha\beta}|^2}{\delta_{\alpha\beta}^2+\frac{\left(\Gamma_\alpha+\Gamma_\beta\right)^2}{4}}, \tag{22}$$

where Γ_α and Γ_β are the energy width of orbitals α and β.

The total NEET rate is calculated by summing over all $M1$ and $E2$ atomic transitions,

$$\lambda^{\mathrm{NEET}} = \sum_{\alpha,\beta}\lambda_{\alpha\to\beta}^{\mathrm{NEET}}. \tag{23}$$

In our thermodynamic domain of interest, between 10^{-3} and $10^{-1}\,\mathrm{g\,cm^{-3}}$, collisional widths are generally the dominant broadening process. Collisional half-widths for an orbital with quantum numbers n and ℓ are estimated using the Dimitrijević and Konjević numerical expression [31–33] and corrected by Peyrusse [34],

$$\Gamma_{n\ell} = N_e\frac{4\pi}{3}\frac{\hbar^3}{m_e^{3/2}}\sqrt{\frac{2\pi}{3}\frac{1}{k_BT}}\left(0.9-\frac{1.1}{Q}\right)\left(\frac{3n}{2Q}\right)^2 \times\left(n^2-\ell^2-\ell-1\right), \tag{24}$$

where N_e is the electronic density, T is the plasma electronic temperature, and Q is the charge state of the ion. For example the collisional half-widths for orbitals $6p_{1/2}$ and $4p_{3/2}$ for a mercury ion with a charge state of 49^+, a plasma temperature of 316 eV, and a density of $10^{-2}\,\mathrm{g\,cm^{-3}}$ are 14 and 8 meV, respectively. The radiative rate of an $E1$ transition from the P shell to the N shell is on the order of a few $10^{12}\,\mathrm{s^{-1}}$. The corresponding width of about 0.6 meV is negligible compared to the collisional widths. At $10^{-3}\,\mathrm{g\,cm^{-3}}$, the domination of the collisions contribution to the total width is not so clear, but it at least gives a minimum effect.

Figure 6 shows the variation of the NEET rate with the temperature (a) and the average charge state (b) in DCA and AAG calculation at $10^{-2}\,\mathrm{g\,cm^{-3}}$ plasma density with $\delta Q = 3$. This ensures that more than 99% of the cumulated probabilities

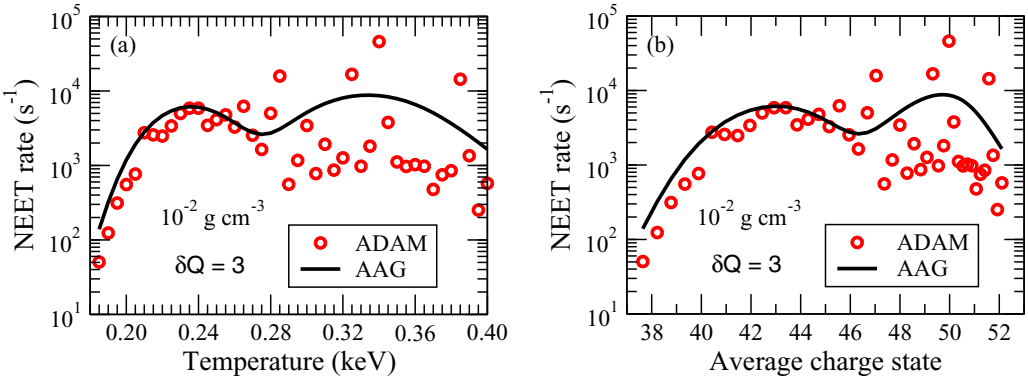

FIG. 6. (Color online) NEET rate with ADAM and AAG models at $10^{-2}\,\mathrm{g\,cm^{-3}}$ as a function of (a) temperature and (b) the average charge state with $\delta Q = 3$.

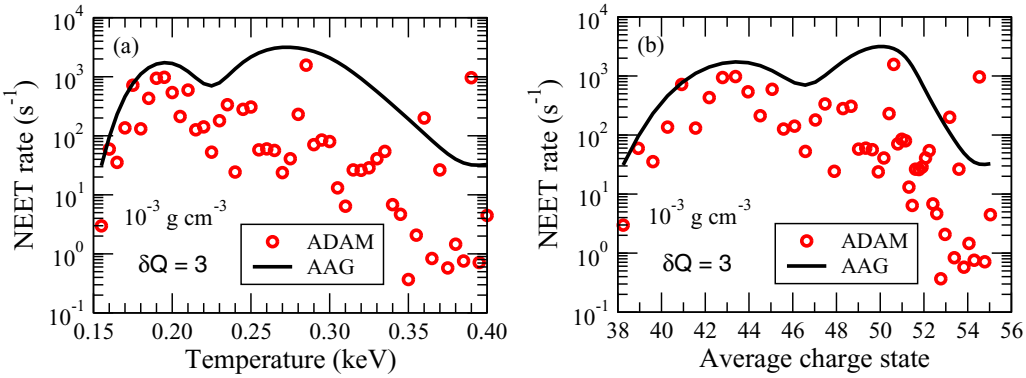

FIG. 7. (Color online) NEET rate with ADAM and AAG models at 10^{-3} g cm^{-3} as a function of (a) temperature and (b) the average charge state with $\delta Q = 3$.

of charge states are taken into account. Two different zones can be distinguished. For a temperature below 260 eV ($\bar{Q} \leqslant 45$), ADAM rates exhibit a nearly continuous behavior close to the AAG rates. The charge is low enough, the total number of transitions between configurations is high, transition energies are separated by amounts smaller than the atomic widths, and overlap between transitions can occur.

Above 260 eV, the ADAM NEET rate exhibits a more erratic behavior. Atomic transitions are less numerous, and overlaps become rarer. Most points are under the AAG rate. NEET rates are now highly dependent on the proximity of the atomic transition energy from the nuclear transition energy.

At the lower density of 10^{-3} g cm^{-3} as shown in Fig. 7, the general behavior on the whole temperature range is the same as occurs for the higher temperatures at 10^{-2} g cm^{-3}. The atomic widths are always lower as their main contributor is still only the collisional width, which is proportional to the density. Adding radiative widths, which are almost independent of density, should not have large consequences on the 10^{-3}-g cm^{-3} behavior. In addition a given charge state requires a lower temperature than for higher density. This induces a lower population of the atomic shells which lowers the number of electronic configurations. Lower atomic widths combined with a lower number of electronic configurations explain a lack of overlap between transitions and ADAM NEET rates further from AAG rates at the highest temperatures.

E. NEET rate variations due to energy uncertainties

A correct evaluation of the NEET rate under specific thermodynamic conditions would require the exact knowledge of both the atomic transition energies and the nuclear transition energy. Here exact means with a precision at least better than collisional widths. However such knowledge is not available and will not be in the foreseeable future. In the case of ^{201}Hg the nuclear transition energy is already known with a very good uncertainty of 1 eV [35]. Therefore, the biggest uncertainty lies in the calculated atomic transition energy. Indeed, the calculation method used in ADAM leads to a variation of the atomic transition energy as a function of the plasma temperature. This variation is not realistic because the energy of an atomic transition depends on the electronic configuration and only very weakly on the plasma temperature. This variation is due to the use of the quantities $\overline{U}_k$ and $\overline{V}_{kk'}$ that outcome from the AAM calculation. Figure 8 shows the variation of the atomic transition energy for two real configurations of the 42^+ and 44^+ charge states as a function of the average charge state of the plasma (which is directly related to the plasma temperature). Transition energies calculated in the CNFM method are also reported.

When the average charge state of the plasma is close to the charge state of the real configuration (42^+ and 44^+) the energy of the atomic transition calculated with ADAM is no more than a few eV away from the CNFM calculation (see Sec. III C).Within a charge state variation of $\delta Q = 3$ the calculated transition energy varies by around 10 eV. This illustrates the uncertainty on the atomic transition energy calculated with the ADAM model. On the other hand, best state-of-the-art atomic physics models, such as the MCDF class of models [26], usually calculate a relative transition energy precision of a few 10^{-3} [25]. This would translate here into a precision of a few eV. From both these uncertainties we

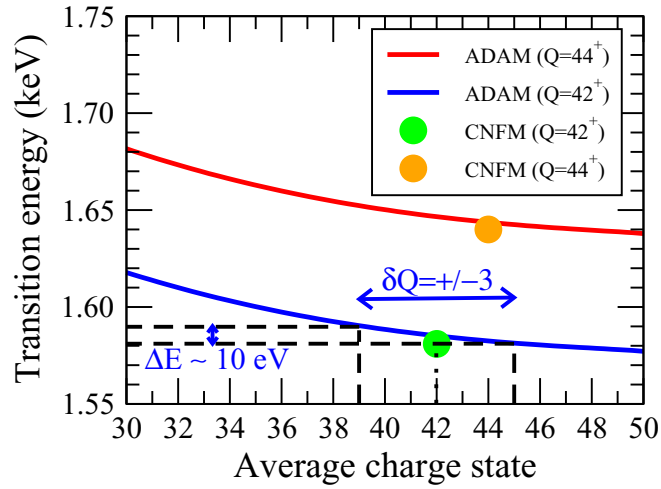

FIG. 8. (Color online) Variation of the $6s_{1/2}$-$4s_{1/2}$ transition energy as a function of the average charge state of the plasma calculated with ADAM. Transitions energies calculated in the CNFM method (see Sec. III C) are also reported.

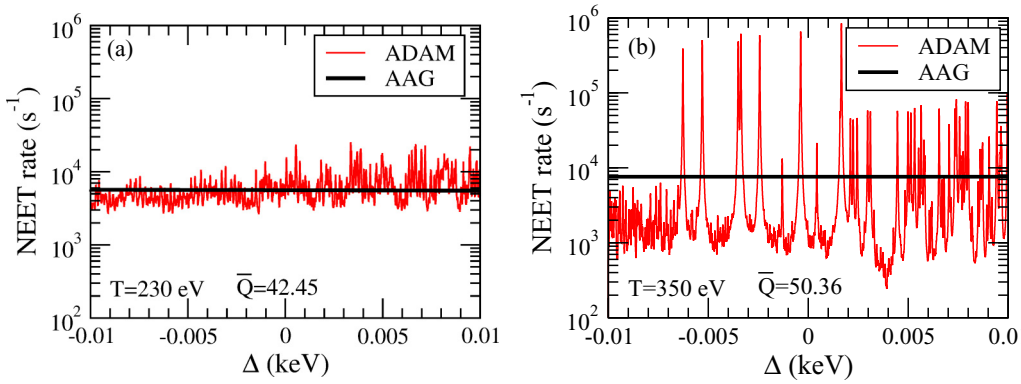

FIG. 9. (Color online) NEET rate as a function of the atomic energy uncertainty Δ for a temperature of (a) 230 eV and (b) 350 eV at 10^{-2} g cm^{-3}.

conservatively adopt a value of 10 eV on the atomic transition energy.

Therefore to get an uncertainty on the NEET rate we must have a look at NEET rate variations within an interval of 10 eV around the mean value of the mismatch,

$$\lambda^{\mathrm{NEET}}_{\alpha\to\beta}(\Delta) = \sum_{C_i^{\alpha\beta}} P\left(C_i^{\alpha\beta}\right)\frac{\Gamma_\alpha}{\hbar}N_\alpha\left(1-\frac{N_\beta}{g_\beta}\right) \times\left(1+\frac{\Gamma_\beta}{\Gamma_\alpha}\right)\frac{|W_{\alpha\beta}|^2}{(\delta_{\alpha\beta}+\Delta)^2+\frac{(\Gamma_\alpha+\Gamma_\beta)^2}{4}}, \quad (25)$$

where Δ is the atomic energy uncertainty parameter [36].

This is shown in Fig. 9 for temperatures of (a) 230 eV and (b) 350 eV and a density of 10^{-2} g cm^{-3}.

As expected from the analysis of Fig. 6, NEET rate fluctuations are much lower at 230 eV ($\bar{Q} = 42.45$) than at 350 eV ($\bar{Q} = 50.36$). Fluctuations remain within an order of magnitude at 230 eV whereas they span over nearly four orders of magnitude at 350 eV. This is confirmed by the NEET rate (more precisely its decimal logarithm) distributions shown in Fig. 10. The NEET rate distribution is narrower at a temperature of 230 eV, and the asymmetry is more pronounced at 350 eV. In this paper, we define a confidence interval as the centered interval spanning exactly 70% of the total distribution. The dashed vertical line is the median value of distribution (50% of the distribution is below and 50% is above). Both straight vertical lines are the boundaries of the confidence interval. The red error bar above the blue curve is the interval as will be plotted in Fig. 11 below.

The amplitude of these fluctuations has been formalized in Fig. 11 for densitoes of 10^{-2} and 10^{-3} g cm^{-3}. For a density of 10^{-2} g cm^2, below 260 eV the ADAM NEET rate exhibits a small uncertainty around a factor of 2, and except for the lowest temperatures, the AAG NEET rate lies within the 70% interval. Compared to the other sources of uncertainties to design an experiment (local thermodynamic equilibrium hypothesis, hydrodynamics . . .) this factor of 2 is low, and the AAG model can be considered as valid for a NEET calculation. For higher temperatures, above 260 eV, the uncertainty gets higher, and the AAG NEET rate only lies at the upper edge of the confidence interval. Above this threshold, it lies above the ADAM average NEET rate by something a little smaller than one order of magnitude. The large uncertainty given by ADAM exhibits a more erratic behavior. At 10^{-3} g cm^{-3}, the ADAM average NEET rate is always smaller than the AAG calculations: around a factor 4 for temperature less than 230 eV up to two orders of magnitudes for the highest temperature.

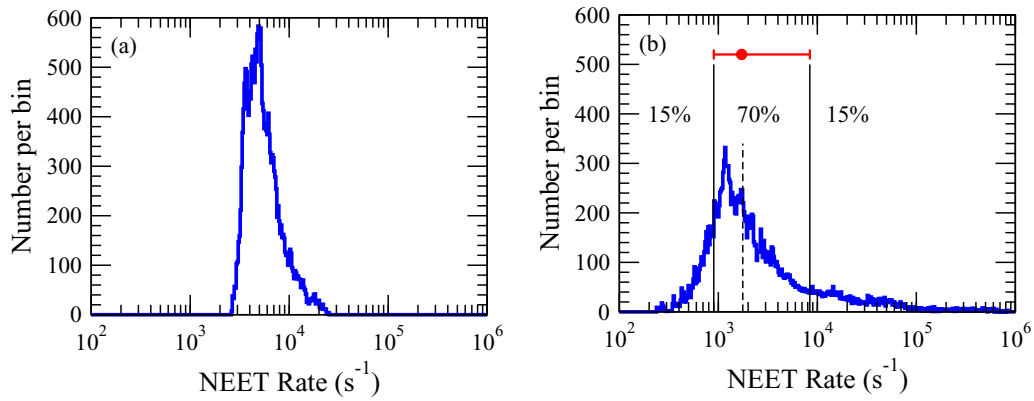

FIG. 10. (Color online) NEET rate distributions for temperatures of (a) 230 eV and (b) 350 eV at 10^{-2} g cm^{-3} with confidence interval superimposed on (b).

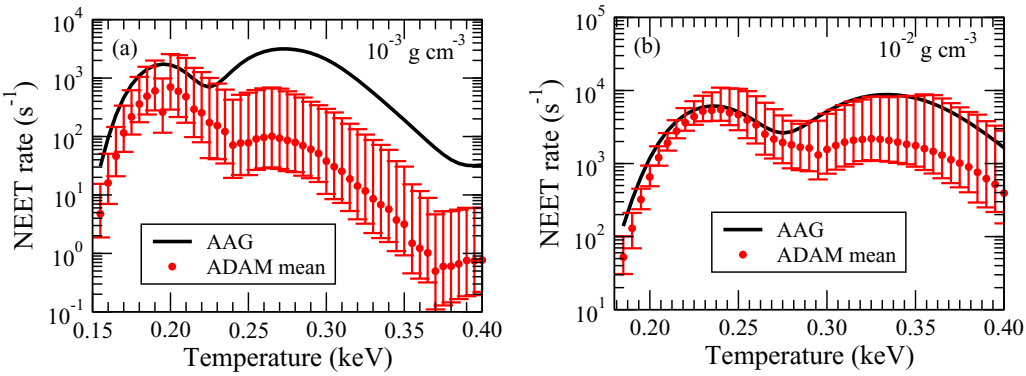

FIG. 11. (Color online) NEET rate fluctuations calculated with the ADAM model at (a) 10^{-3} g cm^{-3} and (b) 10^{-2} g cm^{-3} as a function of temperature.

In the meantime, the uncertainty increases to more than one order of magnitude.

The main issue of the ADAM method is the variation of the transition energy with the plasma temperature. To reduce this effect, it would be possible to use, for each atomic transition and for each real charge state, a potential calculated for the most likely configuration. This would greatly reduce the fluctuations of the ADAM calculation due to this artifact and improve the estimations of the uncertainties around the AAG model.

IV. CONCLUSION

We presented in this paper, the calculation of a NEET rate based on a DCA model. The energy of an atomic configuration has been obtained by a development around the average configuration energy calculated in the framework of the RAAM. The main advantage of this new calculation method, the so-called ADAM model, is to avoid solving the Dirac equation for each configuration. Configurations are selected according to their charge states two or three units away from the average charge state. We have compared a radiative spectrum calculated with the ADAM model and with a calculation where the Hamiltonian for each configuration has been calculated. We have shown that when the average charge state of the plasma is not too far from the charge state of the detailed configuration, the energy of the atomic transition calculated with ADAM is no more than a few eV away from the more realistic calculation.

Using the ADAM model, we succeeded in evaluating variations of the NEET rate around the RAAM value due to the uncertainties on the atomic transition energies. As in our previous works [10,14,15], in the RAAM the influence of the huge number of electronic configurations is taken into account statistically by a Gaussian-shaped broadening around the average transition energy. This continuous approach (AAG) to describe a resonant process may be a severe limitation of this model if the density of the transition energies is not large enough to ensure an overlap between transitions broadened by electronic collisions. We have shown that the ADAM NEET rate exhibits a small fluctuation around a factor of 2 for temperatures less than 260 eV at 10^{-2} g cm^{-3} giving confidence in the AAG calculation in this region. However beyond 260 eV, although both models AAG and ADAM agree within a 70% confidence interval, the ADAM rate exhibits quite large fluctuations making it difficult to conclude on the validity of the AAG within this domain. When the density is lower, the difference between the results of the two models is more important: The average NEET rate of the ADAM code is always smaller than the AAG.

However this study tells us that if the density is greater than 10^{-2} g cm^{-3} we can be confident on the AAG NEET rate calculations for average charge states around 42^{+}. For lower densities, the uncertainty is much higher, and no clear conclusion can be drawn. A more realistic detailed model, taking into account atomic configuration mixing would be required to allow improving the uncertainties around the AAG in the low-density region.

ACKNOWLEDGMENTS

This work was supported by the Contracts No. 20071304005 and No. 20111603003 of the Region Aquitaine, the CEA and the University of Bordeaux.

[1] G. D. Doolen, Phys. Rev. Lett. **40**, 1695 (1978).
[2] G. D. Doolen, Phys. Rev. C **18**, 2547 (1978).
[3] Y. Izawa and C. Yamanaka, Phys. Lett. B **88**, 59 (1979).
[4] V. Méot, J.-C. Baudin, N. Musolino, and C. Camus, Etude de l'excitation de l'235U dans un plasma : l'expérience ISOMERE sur Phébus, CEA, Report No. CEA-R-5944, 2000 (in French) (unpublished).
[5] G. Claverie, M. M. Aléonard, J. F. Chemin, F. Gobet, F. Hannachi, M. R. Harston, G. Malka, J. N. Scheurer, P. Morel, and V. Méot, Phys. Rev. C **70**, 044303 (2004).
[6] F. Gobet, F. Hannachi, M. M. Aléonard, M. Gerbaux, G. Malka, J. N. Scheurer, M. Tarisien, G. Claverie, D. Descamps, F. Dorchies, R. Fedosejevs, C. Fourment, S. Petit, V. Méot, and P Morel, J. Phys. B: At., Mol. Opt. Phys. **41**, 145701 (2008).

[7] M. M. Aléonard, F. Gobet, G. Claverie, M. Gerbaux, F. Hannachi, G. Malka, J. N. Scheurer, M. Tarisien, F. Dorchies, D. Descamps, C. Fourment, S. Petit, V. Méot, and P Morel, J. Mod. Opt. **54**, 2585 (2007).
[8] G. Gosselin, N. Pillet, V. Méot, P. Morel, and A. Y. Dzyublik, Phys. Rev. C **79**, 014604 (2009).
[9] G. Gosselin and P. Morel, Phys. Rev. C **70**, 064603 (2004).
[10] P. Morel, V. Méot, G. Gosselin, D. Gogny, and W. Younes, Phys. Rev. A **69**, 063414 (2004).
[11] S. Kishimoto, Y. Yoda, Y. Kobayashi, S. Kitao, R. Haruki, and M. Seto, Nucl. Phys. **A748**, 3 (2005).
[12] I. Ahmad, R. W. Dunford, H. Esbensen, D. S. Gemmell, E. P. Kanter, U. Rütt, and S. H. Southworth, Phys. Rev. C **61**, 051304 (2000).
[13] S. Kishimoto, Y. Yoda, M. Seto, Y. Kobayashi, S. Kitao, R. Haruki, T. Kawauchi, K. Fukutani, and T. Okano, Phys. Rev. Lett. **85**, 1831 (2000).
[14] G. Gosselin, V. Méot, and P. Morel, Phys. Rev. C **76**, 044611 (2007).
[15] V. Méot, J. Aupiais, P. Morel, G. Gosselin, F. Gobet, J. N. Scheurer, and M. Tarisien, Phys. Rev. C **75**, 064306 (2007).
[16] S. Sakabe, K. Takahashi, M. Hashida, S. Shimizu, and T. Iida, At. Data Nucl. Data Tables **91**, 1 (2005).
[17] B. F. Rozsnyai, Phys. Rev. A **5**, 1137 (1972).
[18] A. L. Ankudinov, A. I. Nesvizhskii, and J. J. Rehr, Phys. Rev. B **67**, 115120 (2003).
[19] T. Blenski, R. Piron, C. Caizergues, and B. Cichocki, High Energy Density Phys. **9**, 687 (2013).
[20] R. D. Cowan, *The Theory of Atomic Structure and Spectra* (University of California Press, Berkeley, 1981).
[21] F. Perrot, Physica A **150**, 357 (1988).
[22] G. Faussurier, C. Blancard, and A. Decoster, Phys. Rev. E **56**, 3488 (1997).
[23] M. Abramowitz and I. Stegun, *Handbook of Mathematical Functions* (Dover, Mineola, NY, 1970).
[24] M. Comet, Ph.D. thesis, 2014 Université de Bordeaux [http://www.theses.fr/2014BORD0458].
[25] D. Denis-Petit, M. Comet, T. Bonnet, F. Hannachi, F. Gobet, M. Tarisien, M. Versteegen, G. Gosselin, V. Méot, P. Morel, J.-C. Pain, F. Gilleron, A. Frank, V. Bagnoud, A. Blažević, F. Dorchies, O. Peyrusse, W. Cayzac, and M. Roth, J. Quant. Spectrosc. Radiat. Transfer **148**, 70 (2014).
[26] J. Bruneau, J. Phys. B: At., Mol. Opt. Phys. **17**, 3009 (1984).
[27] I. P. Grant, Relativistic Quantum Theory of Atoms and Molecules: Theory and Computation, *Springer Series on Atomic, Optical, and Plasma Physics* (Springer-Verlag, New York, 2007).
[28] J. Bruneau, J. Phys. B: At., Mol. Opt. Phys. **16**, 4135 (1983).
[29] I. P. Grant, Adv. Phys. **19**, 747 (1970).
[30] I. P. Grant, J. Phys. B: At., Mol. Opt. Phys. **7**, 1458 (1974).
[31] M. S. Dimitrijević and N. Konjević, J. Quant. Spectrosc. Radiat. Transfer **24**, 451 (1980).
[32] M. S. Dimitrijević and N. Konjević, Astron. Astrophys. **163**, 297 (1986).
[33] M. S. Dimitrijević and N. Konjević, Astron. Astrophys. **172**, 345 (1987).
[34] O. Peyrusse (private communication).
[35] O. Dragoun, V. Brabec, M. Ryšavý, A. Špalek, and K. Freitag, Z. Phys. A **326**, 279 (1987).
[36] M. R. Harston and J. F. Chemin, Phys. Rev. C **59**, 2462 (1999).